Journal of Green Engineering (JGE)

Volume-10, Issue-12, December 2020

Experimental Study of Combined Gusset Plate with Flange Web Cleat Connection in Sustainable,Isolated and Sub-Assemblage of Cold-Formed Steel

[1]Muhammad Firdaus, [2]Anis Saggaff, [3]Mahmood MD Tahir, [4]Shek Poi Ngian, [5]Tan Cher Siang

[1]Civil Engineering Department, Faculty of Engineering, Universitas PGRI Palembang,Indonesia.E-mail:[1]firdaus@univpgri-palembang.ac.id
[2]Civil Engineering Department, Faculty of Engineering, Universitas Sriwijaya, Inderalaya,Indonesia.E-mail:[2]anissaggaf@unsri.ac.id,[6]km73@gmail.com
[3,4,5]Construction Research Centre, Faculty of Engineering, Universiti Teknologi Malaysia,Skudai,JohorBahru,Malaysia.
E-mail: [3]mahmoodtahir@utm.my, [4]shekpoingian@utm.my, [5]tcsiang@utm

Abstract

The characteristic of Cold-Formed Steel (CFS) is its thinness, but it is also a disadvantage because it is more susceptible to buckling. The efforts to improve CFS performance were carried with a variety of research and extended into the joint area. The motivation of the previous researcher's in the connection area was due to limited information in EC3 for gusset plate connections. This paper presents the proposed gusset plate joint combination with flange web cleat angle, which is an innovation from other research, and it was chosen because it can produce extra advantageous in terms of resistance and stiffness. The Isolated Joint Test (IJT) and Sub-assemblage Frame Test (SAFT) were conducted so that the influence of connection could be identified. Four specimens for each procedure and the results showed that the influence of beam dimensions and connection components significantly increased the joint performance, 21% for moment resistance and 47% for

Journal of Green Engineering, Vol. 10_12,13132-13149.

stiffness respectively. The experimental results show that the joint deformation has happened without any failure on the gusset plates, angles and bolts, indicating bearing failure around bolt holes due to the thin plate of the CFS. However, the connection contribution is only a quarter of the ultimate connection capacity in terms of mid-span behaviour. The increment in load capacity, which was not exceeding 1 kN, is mainly controlled by the beam's lateral-torsional buckling. Therefore, the composite beam application is more recommended for CFS so that it can be applied as the primary structure.

Keywords: Cold-formed steel, sub-assemblage, gusset plate, web cleat connection, load capacity.

1 Introduction

Cold-formed steel (CFS) is a new advanced building material which can be a competitive hot-rolled steel (HRS) alternative[1]. The need for CFS is considered to be one of the best economical alternatives and has become the most commonly used material. Since the thickness is not more than 3 mm as stated in [2], this material is often related to as lightweight steel, and yet this is an undeniable truth that the CFS is better than HRS in terms of weight-to-resistance ratio. Because of the advantages, CFS can be recommended as an option to conventional materials such as hot-rolled steel, wood, and stone [3].

The deficiency of CFS, however, is also attributed to the thin plate behaviour, where the plate leads to early buckling or local instability at high-stress levels. Some research on CFS connections were conducted [3] - [13], and the failure mode was shown to be dominated by CFS profiles rather than connection. In order to enhance lightweight ductility, flange sections were tightened from flat to curve, together with an out-off plane stiffener on the beam web [13] - [17].

Light steel testing was further developed into the connection area; some of the studies were driven by the type of connection not yet available in EC3. Bucmys argued that the connection must be constructible easily. In contrast, a gusset plate connection was suggested, and the rigidity of the gusset plate is largely related to the design instructions not available in EC3[10]. However, due to thinness of CFS, the influence of elongation of bolt holes on rigidity and connection resistance must be considered [18].

This paper presents experimental results of haunched gusset plate's connection that beyond of Bucmys's research. Combined with flange web cleat angle section, which has the purpose of increasing the connection resistance, and as reinforcement without having to disassemble the existing construction [19], [20]. M12 bolts grade 8.8 were used as a fastener, and it is very suitable for light steel profiles.

The specimens were tested under monotonic loading until failure mode was detected. Isolated joint test (IJT) procedures were conducted to investigate the connection behaviour, whereas sub-assemblage frame test (SAFT) was conducted to identify the connection as part of the portal frame.

2 The Material and Methods

2.1 Material Properties and Specimen

Four specimens were tested in this study, two samples for isolated joint test (IJT) and two for sub-assemblage frame test (SAFT). The suggested connection is presented in Figure 1, the double lipped channel (DLC) of lightweight steel was used and connected with M12 bolts back to back, forming an I shape. This arrangement makes the axis of channel section becomes symmetrical so that it is stronger against torsional buckling. The details of material for both IJT and SAFT are summarised in Table 1 and table 2.

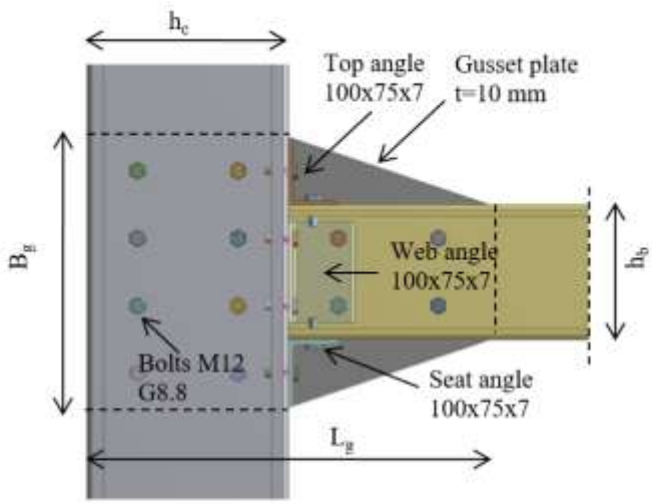

Figure 1 The combination gusset plate and flange web cleat connection

Table 1 Details of Material for Ijt Specimens

TEST ID	IJT-07	IJT-08	Note	Grade
Beam	DLC200	DLC250	L=1.1 m	S350GD+Z
Column	DLC300	DLC300	L=3 m	S350GD+Z

Gusset Plate	400x600	550x600	t=10 mm	S350
Web Angle	L100x75x7	L100x75x7		S350
Seat Angle	L100x75x7	L100x75x7		S350
Bolt	M12	M12		Grade 8.8

Table 2 Details of Material for Saft Specimens

TEST ID	SAFT-07	SAFT-08	Note	Grade
Beam	DLC200	DLC250	L=4 m	S350GD+Z
Column	DLC300	DLC300	L=3 m	S350GD+Z
Gusset Plate	400x600	550x600.	t=10 mm	S350
Web Angle	L100x75x7	L100x75x7		S350
Seat Angle	L100x75x7	L100x75x7		S350
Bolt	M12	M12		Grade 8.8

Hot rolled haunched gusset plate was used to distribute the concentrated force from beam to the column. The haunched shape was chosen because it allows the placement of more bolts on the web column, thereby increasing the strength and stiffness of the connection. The bolt holes were measured to 13 mm to prevent a sudden drop of the specimens. The thickness of 10 mm was selected and is expected to provide sufficient resistance and to delayed buckling on the gusset plate. M12 bolts were arranged not beyond the validity range requirements of EC3 [21]. The dimensions and size of the gusset plates are shown in Fig. 2 and Table III

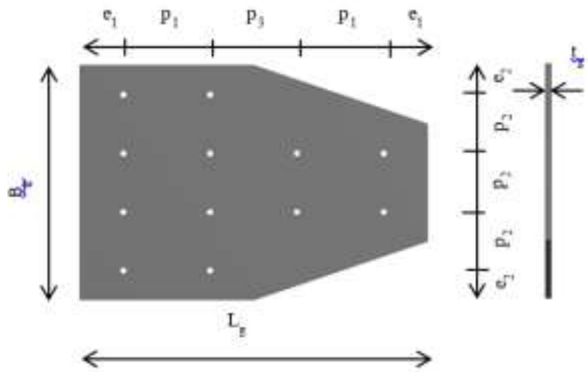

Figure 2 Haunched gusset plate dimension and bolt hole position

Table 3 Details of Gusset Plate Dimensions

Remarks	IJT-07 SAFT-07	IJT-08 SAFT-08	Unit
Bg	400	550	mm
Lg	600	600	mm
e1	75	75	mm
e2	50	50	mm
p1	150	150	mm
p2	100	100	mm
p3	150	150	mm

2.2 Method

Full-scale tests on IJT and SAFT were conducted at the Universiti Teknologi Malaysia (UTM) Construction Research Centre (CRC), with the following procedure as described below.

2.2.1 Isolated Joint Test

The isolated joint test is conducted to acquire the characteristics of the connection in the form of a moment-rotation. The bending moment will be generated from the load cell placed at 1000 mm from the face of the column as in Figure 3. The distance is considered sufficient to represent of contra flexural position between the negative moment of the connection and the positive moment of the beam. Two inclinometers were positioned at the centre line of the beam (I-1) and column (I-2), so the rotation of connection can be determined by Eq. (1):

$$\phi = \frac{\phi_{Beam} - \phi_{Column}}{180} . \pi \qquad (1)$$

Five LVDT (L-1 to L-5) were used to obtain the deformation according to the orientation of the instrument. Point load was given with incremental of 0.2 – 0.5 kN. The specimens were unloaded after 25% of the design load was reached, then reloaded. The aim is to find out the initial stiffness of the connection. The load is continuously increased by force control until a significant deflection has happened without an increase in load. From this forward, the experiment is monitored by the displacement control with increments of 5 mm until the failure mode was noticeable. Figure 4 presents the installed specimens inside frame rig.

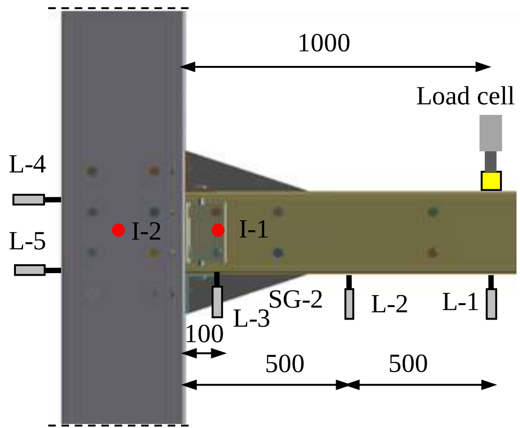

Figure 3 Full scale isolated joint test (IJT) arrangement

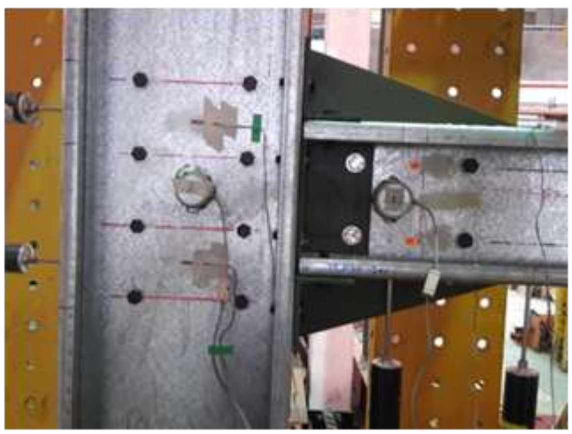

Figure 4 Installed specimens of IJT inside frame rig

2.2.2 Sub-assemblage Frame Test

The SAFT experimental test is measured using the method of the beam organizational efficiency to the applied strength and the capacity of the operation. The beam's mid-span behaviour that is connected to the beam's maximum deflection could only be recognised by implementing the lateral restriction at the beam's L/4 span. As illustrated in Fig. Fifth, at the top of the beam, the spreader beam with a length of 2.1 metres was positioned to extend the concentrated load from the hydraulic jack to the top of the beam flange. Two Inclinometers (I-1 and I-2) were placed in the same position as IJT. A total of seven LVDT (L-1 to L-7) were installed, as indicated in Figure 5. The beam deflection is obtained from L-1 which is placed in the mid-span, L-2 and L-3 which are placed L/4 span just below the spreader beam's support. Unloaded and reloaded procedures were also carried out on this test with the

same purpose as the IJT test. The test object after it was installed in the frame rig, as shown in Figure 6.

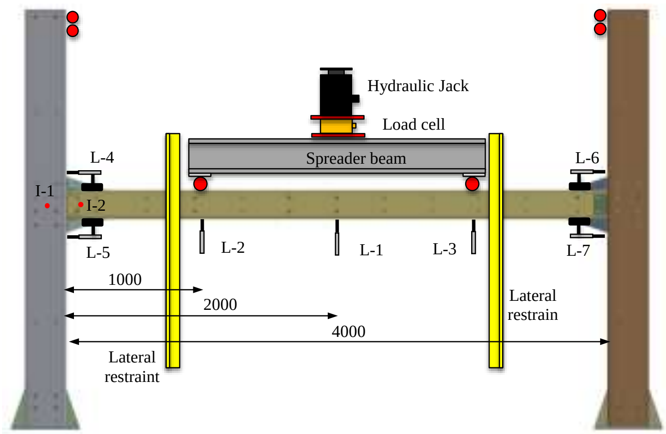

Figure 5 Full-scale sub-assemblage frame test arrangement

Figure 6 Installed specimens of SAFT inside frame rig

3 Result and Discussion

3.1 Failure mode of Isolated Joint Test

The failure mode of the joints is visible by the flexural of column flange for both specimens IJT-07 and IJT-08 (Figure 7 and Figure 8). Since the highest tensile loads emerge at the stress zone, the loss occurred and the seat angle drives the column flange at once into the compression zone. In the compression field, the presence of heavy workloads causes the column flanges to be locally buckled.

The rotation of the gusset plate is also detected, resulting in excessive stress on the bolt and bolt hole.

On the gusset plate and angle part, there is no buckling loss, or bolt shear loss. Thus, it is indicated that a bearing failure of CFS resulted in joint deformation. The shape of deformation is a shred of evidence that CFS thickness is the weakest component due to thin plate behaviour.

3.2 Moment-rotation of Isolated Joint Test

The gradient shift shows that an increase or decrease in the tolerance of the instant caused by interaction between the elements of the link. As shown in Figure 9 and Figure 10, at the initial phase, the bolts are still tightened, characterized by a height gradient. Continued by the second stage, in which the shift of the bolt shank touches the bolt hole, leading to a lower gradient. The third stage, the increase of gradient happens when the bolts at the top angle start to contribute, and seat angle starts to 'push' the column web at the compression zone. The rotation of the gusset plate also occurs due to elastic deformation of the bolt. The fourth stage, the gradient becomes plateau or decrease significantly when the ultimate load has exceeded the joint capacity, or excessive deformation occurs at the beam end.

Figure 7 The failure mode of IJT-07

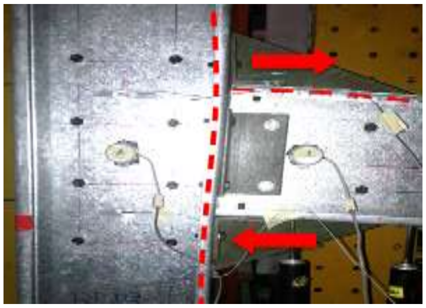

Figure 8 The failure mode of IJT-08

The stiffness of joint for IJT-07 is Sj = 640 kNm/rad, and the maximum moment resistance is 37 kNm as in Fig 9. IJT-08 specimens give the stiffer connection with Sj = 960 kNm /rad and Mj = 43 kNm as in Fig 10. The rotational at the final load is 0.063 rad and 0.05 rad for IJT-07 and IJT-08, respectively. As the rotation is more than 0.03 rad[22], the link may be known as a ductile connection. It could be concluded, IJT-08 is stronger 21% and stiffer 47% than IJT-07, the increase in joint resistance due to the influence of the dimensions of the beam and gusset plates.

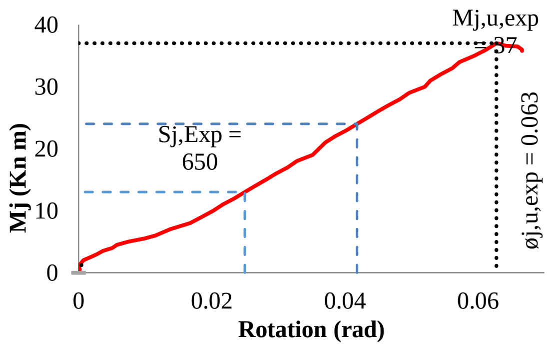

Figure 9 Moment-rotation for IJT-07

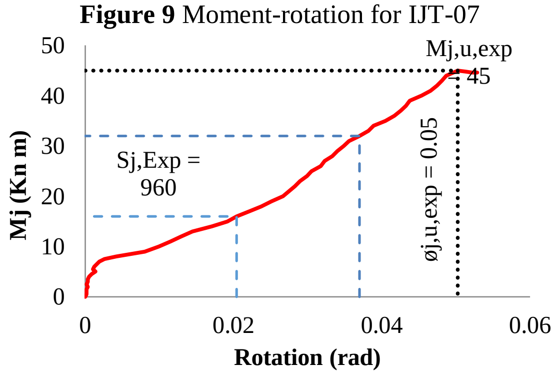

Figure 10 Moment-rotation for IJT-08

3.3 Sub-assemblage Frame Test

3.3.1 Failure mode

Failure mode usually occurs at the mid-span of the beam, starting with the creation of a wave pattern at the top flange of the beam (red dashed line in Figure , Figure 11), and finish after the beam flange experiences local buckling accompanied by torsional buckling (Figure 12). Although the beam depth was used is different, the final load for two specimens was almost the same with 98.3 kN (SAFT-07) and 98.9 kN (SAFT-08) respectively. The loss of the top flange of the beam is fact of the need for inclusive model to remove torsional loss in semi-continuous beams, specifically when CFS is

used for the main beam.

Figure 11 Development of wave pattern for SAFT-07

Figure 11 Development of wave pattern for SAFT-08

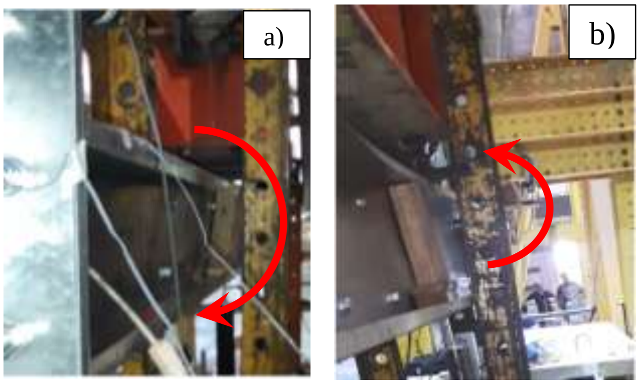

Figure 12 Lateral torsional buckling: a) SAFT07 and b) SAFT-08

3.3.2 Load deflection

Load-deflection of mid-span of the beam was taken from LVDT L-1 and presented in Figure 13, and Figure 14. The relationship between load and deflection is linear at the initial state and followed by non-linear behaviour after the load is increased. The specimen is failed indicated by a decrease of slope and then plateau at the ultimate load. For SAFT-07, the maximum deflection at mid-span is 33.49 mm with the final load of 98.30 kN. While for SAFT-08 the deflection is lower with 22 mm and the ultimate load of 98.90 kN.

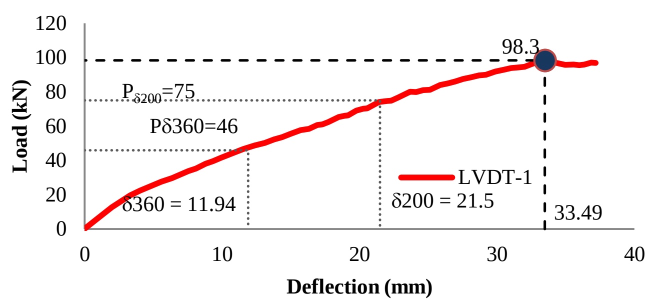

Figure 13 Load-deflection of SAFT-07

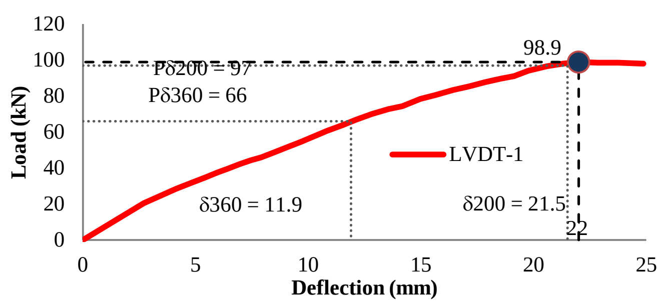

Figure 14 Load-deflection of SAFT-08

The construction has to comply with the serviceability requirements that refer to the maximum permissible deflection. According to Hejazi and Chun [23], the first criteria of vertical deflection limit is L/360 = (4000 +300)/360 = 11.94 mm, where L is the distance for both centreline of the columns. The second deflection limits is L/240 = 4300/200 = 21.25 mm. The summary of maximum loading and deflection of the specimens are presented in Table . For example, SAFT-07 the maximum deflection about 67.12 mm that exceeds allowable deflection. From the Load-deflection graph, it can be seen that the maximum load allowed is 75 kN for L/360 and 46 kN for L/200. The failure mode is Lateral torsional buckling (LTB).

Table 4 Summary of Load-Deflection for Saft Tests

Remarks	SAFT-07	SAFT-08	Unit
P_{max}	98.30	98.90	kN
δ_{max}	33.49	22.00	mm
$\delta_{(L/360)}$	11.94	11.94	mm
$P(_{L/360)}$	46	66.00	kN
$\delta_{(L/200)}$	21.50	21.50	mm
$P_{(L/200)}$	75	97	kN
Failure	LTB	LTB	

3.3.3 Load rotation

The rotation was obtained from the inclinometer and calculated by using Eq. (1). Load-rotation curves for the connections are shown in Figure 15 and Figure 16. The rotation ultimate for SAFT-07 is achieved with 0.018 radians, while SAFT-08 produced stiffer connection with lower rotations of 0.011 radians at the end of the experimen.

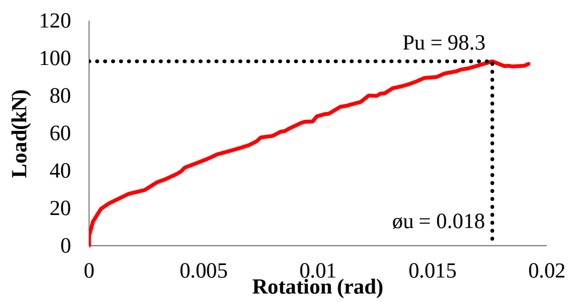

Figure 15 Load-rotation of SAFT-07

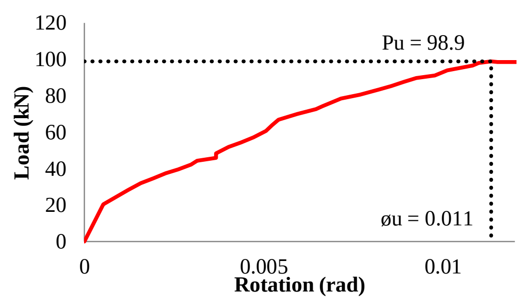

Figure 16 Load-rotation of SAFT-08

3.3.4 Moment Resistance

The moment of resistance (Mj) of the SAFT relation cannot be explicitly defined. However, as in[24] moment resistant, as per Tahir, et al., it could be

measured by analyzing beam rotation at full load from the sub-assembly test with the moment rotation curve from the findings of the isolated joint test.

For example, from the Load-deflection and P-rotation graph for SAFT-07 (Figure 13 and Figure 15), the ultimate load is Pu = 98.3 kN and the rotation of ϕu = 0.018 rad. Furthermore, employing the moment-rotation graph from the isolated joint test (Figure 17), for 0.018 radians, the moment of joint Mj = 7.3 kNm is obtained. With the same procedure, for SAFT-08 the moment of joint Mj is 10.5 kNm.

The analysis for SAFT-08 is performed with the same procedure, the result is $M_{beam,SAFT-08}$ = 38.95 kNm that lower than SAFT-07. For SAFT-07, from Fig. 18 the ratio between Mj = 8.2 to Mj,u = 37 is 0.22, and SAFT-08 is slightly larger at 0.23. This shows from the results of the sub-assemblage test; the connection only contributes 22% and 23%, which means it only reaches less than a quarter of the connection moment resistance from the IJT test.

Refer to Figure 17, the joint moment ratio of Mj=8.2 and Mj,u=37 is 0.22 for SAFT-07, and the ratio for SAFT-08 is slightly higher at 0.23, as seen in Figure 18. The results show that from the sub-assemblage tests, the connection only contributed 22% and 23%, which means it only reached less than a quarter of the moment resistance from the cantilever beam test.

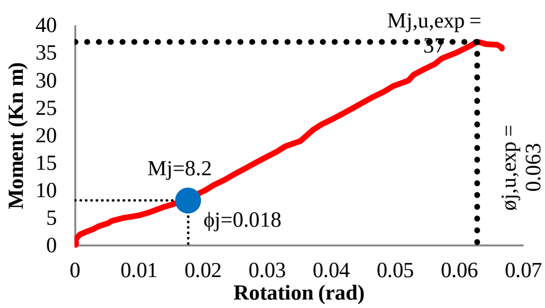

Figure 17 Moment of joint for SAFT-07

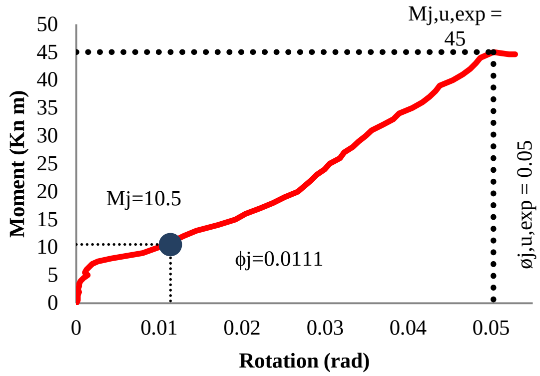

Figure 18 Moment of joint for SAFT-08

The greatest moment of the beam is determined by the stiffness of the joint in semi-continuous construction. As the joint stiffness rises, the positive moment in the mid-span declines and vice versa. Figure 19 shows the influence the moment of the joint to the mid-span bending moment of the beam. In the case of SAFT-07, the bending moment calculation is presented below.

L= 4 m
L_1 = 1 m
P= 98.30 kN
M_j = 8.2 kNm

Bending moment
$M_{max,SAFT-07} = 0.5\ P\ L_1 = 49.155$ kNm
$M_{beam,SAFT-07} = M_{max,SAFT-07} - M_j = 40.95$ kNm

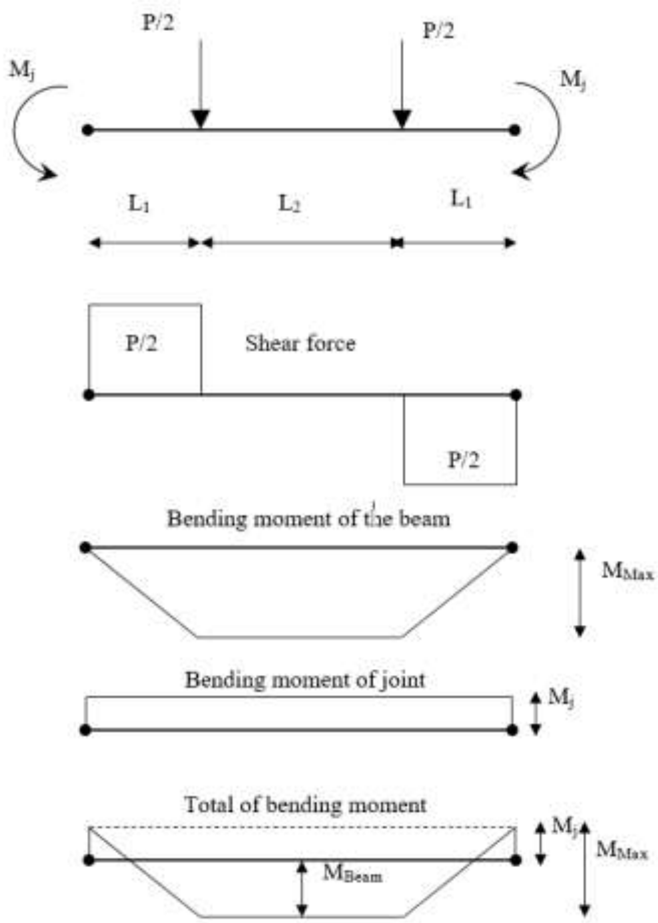

Figure 19 Bending moment diagram at the beam

4 Conclusions

The investigation of combined gusset plate joint with flange web cleat has been carried out. Based on the outcomes acquired, several observations were produced, which led to the following findings. The deformation at the joint area in the isolated joint tests shows that the flexural pattern on the column flange demonstrates a properly stiff connection. The local buckling of the column flange was happened, even though it has been reinforced employing the seat angle. The IJT test results show the effect of beam dimensions and gusset plates increased the moment resistance 21% and stiffness 47%.

The sub-assemblage test exhibits an insignificant increase in load on both sub-assemblage (i.e. SAFT-07 and SAFT-08). The difference is not more than 1 kN. The contribution of connection is less than 23% leads to the maximum bending moment at the beam. Consequently, the mid-span deformation is more than allowable deflection of L/360 and L/240 before the moment ultimate of the joint was reached. It is concluded, the absence of a failure mode in the joint area is the indications of the CFS application in a portal frame is limited by the resistance of lightweight beam itself, particularly in lateral-torsional buckling. It is confirmed that composite application is highly recommended for CFS as part of a portal frame. The research on isolated and sub-assemblage composite connections by applying CFS is required.

Acknowledgement

The authors gratefully thank Universitas Sriwijaya and Construction Research Center of Universiti Teknologi Malaysia (UTM-CRC) for funding this research under grant number 345. Special thanks and sincere gratitude to Prof. Anis Saggaff and Prof. Mahmood Md. Tahir for helpful guidance and assistance.

References

[1]C. Yu., "Recent Trends in Cold-formed Steel Construction", Woodhead Publishing, 2016.
[2]D. Dubina., V. Ungureanu., R. Landolfo., "Design of Cold-formed Steel Structures: Eurocode 3: Design of Steel Structures", Wiley, 2012.
[3]Y. Lee., C. Tan., S. Mohammad., J. Lim., R. Johnston., "Numerical study of joint behaviour for top-seat flange cleat connection in cold-formed steel structures", Scientia Iranica. Transaction B, Mechanical Engineering, Vol.22, no.4, pp.1554-1566, 2015.
[4]R. U. Kulsum, Nadya., F. Usman., "An Experimental Analysis on the Moment Rotation of Beam-Column Connection using Cold-form Steel

Section", International Journal of Engineering & Technology, Vol.7, no.4.35, 2018.
[5]Ž. Bučmys., A. Daniūnas., J.-P. Jaspart., J.-F. Demonceau., "A component method for cold-formed steel beam-to-column bolted gusset plate joints", Thin-Walled Structures, Vol.123, pp.520-527, 2018.
[6]M. Firdaus., A. Saggaff., M. M. Tahir., "Finite element analysis of composite beam-to-column connection with cold-formed steel section", AIP Conference Proceedings, Vol.1903, no.1, 2017.
[7]Ž. Bučmys., A. Daniūnas., "Rectangular gusset plate behaviour in cold-formed I-type steel connections", Archives of Civil Engineering, Vol.63, no.2, 2017.
[8]T. C. Siang., M. Md., M. Muhammad., "Experimental Investigation of Bolted Angle Joints for Cold formed Steel with Double Channel

Sections", Proc. of the Third Inti. Conf. Advances in Civil ,Structure and Mechanical Engineering, -CSM, pp. 14-17, 2015.
[9]Y. H. Lee., C. S. Tan., S. Mohammad., Y. L. Lee., "Mechanical Properties Prediction for Cold-formed Steel Angle Connection with Various Flange Cleat Thickness", JURNAL TEKNOLOGI,,Vol.74, no.4, pp. 51-59, 2015.
[10]Ž. Bučmys., A. Daniūnas., "Analytical and experimental investigation of cold-formed steel beam-to-column bolted gusset-plate joints", Journal of Civil Engineering and Management, Vol.21, no.8, pp.1061-1069, 2015.
[11]C. Tan., et al., "Numerical simulation of cold-formed steel top-seat flange cleat connection", Jurnal Teknologi, Vol.61, no.3, pp.63-71, 2013.
[12]Y. H. Lee., C. S. Tan., Y. L. Lee., M. M. Tahir., S. Mohammad., P. N. Shek., "Numerical Modelling of Stiffness and Strength Behaviour of Top-Seat Flange-Cleat Connection for Cold-Formed Double Channel Section", Applied Mechanics and Materials, Vol.284-287, pp.1426-1430, 2013.
[13]A. Bagheri, Sabbagh., M. Petkovski., K. Pilakoutas., R. Mirghaderi., "Cyclic behaviour of bolted cold-formed steel moment connections: FE modelling including slip", Journal of Constructional Steel Research, Vol.80, pp.100-108, 2013.
[14]E. M. Hassan., M. H. Serror., S. A. Mourad., "Numerical prediction of available rotation capacity of cold-formed steel beams", Journal of Constructional Steel Research, Vol.128, pp.84-98, 2017.
[15]A. Bagheri, Sabbagh., M. Petkovski., K. Pilakoutas., R. Mirghaderi., "Ductile moment-resisting frames using cold-formed steel sections: An analytical investigation", Journal of Constructional Steel Research, Vol.67, no.4, pp.634-646, 2011.
[16] S.Das and J.K. Prasad Yuvaprakash J, P. Kumar,"Experimental And Numerical Studies On Double Delta Wing With Sharp Leading Edge At Subsonic Speed",International Research Journal of Multidisciplinary Science & Technology (IRJMRS),Vol.1,no.3,pp.132-145,2016.

[17] K.Thiagarajan and N.Umamaheswari,"Numerical Investigation on Pull-Out Response of Steel Fibers in Concrete - A Sustainable Approach", Journal of Green Engineering, Vol.10, no.9,pp.5057–5075,2020.
[18]Z. Nagy, A. Dező, and R. Ballok, "Application of the component method for cold formed joints assisted by finite element analysis", Eighth International Conference on THIN_WALLED STRUCTURES(ICTWS), pp.1-18, 2018.
[19]J. Reinosa., A. Loureiro., R. Gutierrez., M. Lopez., "Analytical frame approach for the rotational stiffness prediction of beam-to-column angle connections", Journal of Constructional Steel Research, Vol.106, pp.67-76, 2015.

[20]Z. Kong., S.-E. Kim., "Moment-rotation behavior of top-and seat-angle connections with double web angles", Journal of Constructional Steel Research, Vol.128, pp.428-439, 2017.
[21]BS EN 1993-1-8 -" Eurocode 3: Design of steel the Part 1-8: Design of joints", 2005.
[22]C. Bernuzzi., B. Cordova., "Structural Steel Design to Eurocode 3 and AISC Specifications", John Wiley & Sons, 2016.
[23]F. Hejazi., T. K. Chun., "Steel Structures Design Based on Eurocode 3", Springer, 2018.
[24]M. M. Tahir., A. Sulaiman., and A. Saggaff., "Structural Behavior of Trapezoidal Web Profiled Steel Beam Section using Partial Strength Connection," Electronic Journal of Structural Engineering, Vol.8, pp.55-66, 2008.

Biographies:

Muhammad Firdaus, Civil Engineering Department, Faculty of Engineering, Universitas PGRI Palembang,Indonesia.

Anis Saggaff, Civil Engineering Department, Faculty of Engineering, Universitas Sriwijaya, Inderalaya,Indonesia.

Mahmood MD Tahir, Construction Research Centre, Faculty of Engineering, Universiti Teknologi Malaysia,Skudai,JohorBahru,Malaysia.

Shek Poi Ngian, Construction Research Centre, Faculty of Engineering, Universiti Teknologi Malaysia,Skudai,JohorBahru,Malaysia.

Tan Cher Siang, Construction Research Centre, Faculty of Engineering, Universiti Teknologi Malaysia,Skudai,JohorBahru,Malaysia.